

Selective Extraction of Americium(III) over Europium(III) with the Pyridylpyrazole Based Tetradentate Ligands: Experimental and Theoretical Study

Jieru Wang,[†] Dongping Su,[†] Dongqi Wang,[‡] Songdong Ding,^{*,†} Chao Huang,^{*,†} Huang Huang,[†] Xiaoyang Hu,[†] Zhipeng Wang,[†] and Shimeng Li[†]

[†]College of Chemistry, Sichuan University, Chengdu 610064, P.R. China

[‡]Multidisciplinary Initiative Center, Institute of High Energy Physics, Chinese Academy of Sciences, Beijing 100049, P.R. China

Supporting Information

ABSTRACT: 1,3-Bis[3-(2-pyridyl)pyrazol-1-yl]propane (Bipp) and 1,2-bis[3-(2-pyridyl)pyrazol-1-methyl]benzene (Dbnpp), the pyridylpyrazole based tetradentate ligands, were synthesized and characterized by MS, NMR, and FT-IR. The solvent extraction and complexation behaviors of Am(III) and Eu(III) with the ligands were investigated experimentally and theoretically. In the presence of 2-bromohexanoic acid, the two ligands can effectively extract Am(III) over Eu(III) and other rare earth(III) metals (RE(III)) in HNO₃ solution with the separation factors ($SF_{Am/RE}$) ranging from 15 to 60. Slope analyses showed that both Am(III) and Eu(III) were extracted as monosolvated species, which agrees well with the results observed from X-ray crystallography and MS analyses. The stability constants ($\log K$) obtained from UV–vis titration for Eu(III) complexes with Bipp and Dbnpp are 4.75 ± 0.03 and 4.45 ± 0.04 , respectively. Both UV–vis titration and solvent extraction studies indicated that Bipp had stronger affinity for Eu(III) than Dbnpp, which is confirmed by density functional theory (DFT) calculations. DFT calculations revealed that the $AmL(NO_3)_3$ ($L = Bipp$ and $Dbnpp$) complexes are thermodynamically more stable in water than their Eu(III) analogues, which is caused by greater covalency of the Am–N than Eu–N bonds. Theoretical studies gave an insight into the nature of the M(III)–ligand bonding interactions.



INTRODUCTION

The minor actinides (An), such as Am(III) and Cm(III), are the main contributors to the long-term radiotoxicity of high level liquid waste (HLLW) issued from the PUREX process.¹ For reducing the load to the repository of HLLW, An(III) should be converted into the short-lived or stable nuclides by transmutation.² However, the bulk of lanthanides(III) (Ln(III)) in HLLW can absorb neutrons effectively and therefore prevent the transmutable An(III) capturing neutrons.³ For a good transmutation, it is very necessary to separate An(III) from Ln(III).

An(III)/Ln(III) separation is a challenging task because of the same oxidation state and very similar properties. According to the principle of hard and soft acids and bases,⁴ both An(III) and Ln(III) belong to “hard” ions, but An(III) are slightly softer than Ln(III).⁵ Thus, An(III)/Ln(III) separation can be carried out by selective extraction employing the soft ligands, e.g. S-donor and N-donor heterocyclic ligands.⁶ Up to now, these extractants, such as bis(2,4,4-trimethyl-pentyl)-dithiophosphinic acid,⁷ bis(chlorophenyl)dithiophosphinic acid,⁸ 2,6-bis(5,6-dialkyl-1,2,4-triazin-3-yl)pyridines (BTPs),⁹ 6,6'-bis(5,6-dialkyl-1,2,4-triazin-3-yl)-2,2'-bipyridines

(BTBPs),¹⁰ and 2,9-bis(1,2,4-triazin-3-yl)-1,10-phenanthroline (BTPHens)¹¹ (see Figure 1), have been widely studied. Unfortunately, they suffered from poor chemical and irradiation stability, relatively slow extraction kinetics, as well as difficulties of synthesis, resulting in their unsuitable uses in practical processes. Thus, great efforts still need to be made to explore more efficient extractants for An(III)/Ln(III) separation.

In recent years, it was found that the ligands composed of pyridine and pyrazole exhibited good effectiveness for An(III)/Ln(III) separation. Earlier studies showed that 6-(3,5-dimethyl-1-H-pyrazol-1-yl)-2,2'-bipyridine (dmpbipy; see Figure 1) with 2-bromohexanoic acid could selectively extract Am(III) over Eu(III) in HNO₃ solution.¹² The separation factor ($SF_{Am/Eu}$) could reach 8 at pH 2.4, showing an extraction selectivity for Am(III) to some extent. But the $SF_{Am/Eu}$ values obtained are not high enough to meet the needs of practical applications. Shortly afterward, Bremer et al. made some modifications on dmpbipy; that is, one of the pyridyl rings of dmpbipy was substituted by a five membered pyrazolyl ring, and synthesized

Received: June 28, 2015

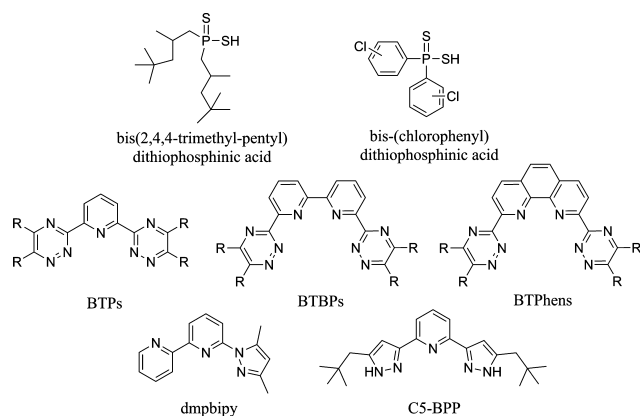


Figure 1. Chemical structures of the representative ligands for An(III)/Ln(III) separation.

2,6-bis(5-(2,2-dimethylpropyl)-1H-pyrazol-3-yl)pyridine (C5-BPP; see Figure 1). In the presence of 2-bromohexanoic acid, C5-BPP gave a $SF_{Am/Eu}$ of 100 at 0.1 mol/L HNO_3 .¹³ As far as $SF_{Am/Eu}$ is concerned, it can attain levels nearly as high as BTPs, suggesting a favorable prospect of application for An(III)/Ln(III) separation. In an attempt to clarify the molecular origin of the selectivity of C5-BPP for Am(III), Adam et al. prepared ^{15}N labeled C5-BPP as well as its complexes with Am(III) and Ln(III) (La, Sm, Yb, Lu, and Y), and then they investigated the bonding of C5-BPP with the metal ions by ^{15}N NMR spectroscopy.¹⁴ Compared with Ln(III) complexes, the chemical shifts for coordinated N atoms in the Am(III) complex are larger. These indicated that metal–ligand (M–L) bonding in the Am(III) complex was more covalent than that in Ln(III) complexes. Thus, C5-BPP exhibited excellent selectivity for Am(III). More notably, in contrast to BTPs, the pyridylpyrazole based ligands have fewer numbers of N atoms in the heterocycle, which may be favorable for chemical and irradiation stability. Besides that, their syntheses are relatively easy. In a word, as the promising extractants for An(III)/Ln(III) separation, the pyridylpyrazole based ligands are definitely worth exploring. But it is regrettable that there are few reports on this new kind of N-donor heterocyclic ligands. For further developing new efficient N-donor heterocyclic extractants based on the pyridylpyrazole ligands, it is essential to understand their fundamental extraction and complexation behaviors of An(III) and Ln(III) experimentally and theoretically.

In the present paper, we designed and synthesized two representative pyridylpyrazole based tetradentate ligands. One is 1,3-bis[3-(2-pyridyl)pyrazol-1-yl]propane (Bipp), and the other is 1,2-bis[3-(2-pyridyl)pyrazol-1-methyl]benzene (Dbnpp). In their chemical structures, the two pyridylpyrazole groups are linked through an aliphatic and aromatic bridge, respectively. The extraction behaviors of Am(III), Eu(III), and other rare earth ions(III) (RE(III)) were investigated by a system of the ligands and 2-bromohexanoic acid in *tert*-butyl benzene (TBB). The single crystal of Bipp with Eu(III) was also obtained and characterized. The stability constants ($\log K$) for Eu(III) with the ligands were determined by UV–vis titration. The extraction model and complexation of the ligands with Am(III) and Eu(III) were studied by density functional theory (DFT) calculations.

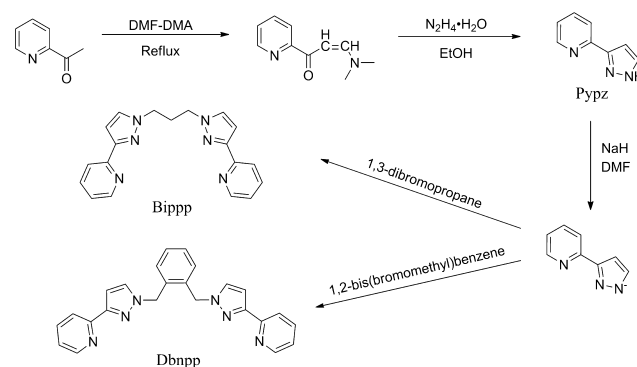
EXPERIMENTAL SECTION

General. All chemical reagents were of AR grade without purification. Solutions of $RE(NO_3)_3$ ($RE = La, Ce, Pr, Nd, Sm, Eu, Gd, Tb, Dy, Ho, Er, Tm, Yb, Lu, and Y$) in diluent HNO_3 were prepared from their oxides (99.99%, Aldrich). The tracer stock solution of ^{241}Am in 0.1 mol/L HNO_3 solution was provided by China Institute of Atomic Energy (CIEA).

UV–vis spectra were performed with a PERSEE TU-1810 spectrophotometer. FT-IR spectra were measured on a Nicolet Nexus 670 model instrument. NMR spectra were recorded on a Varian Inova 400 MHz NMR spectrometer using $CDCl_3$ with tetramethylsilane as an internal standard. MS spectra were obtained on a LCMS-2T-TOF spectrometer. Single-crystal X-ray diffraction measurements were carried out using an Agilent Technologies Gemini diffractometer.

Synthesis. Bipp and Dbnpp were synthesized according to Scheme 1. 3-(2-Pyridyl)pyrazole (Pypz) was prepared referring to the literature.¹⁵

Scheme 1. Synthesis Route of Bipp and Dbnpp



To a solution of Pypz (3.0 g, 20 mmol) in 100 mL of DMF was added NaH (1.2 g, 50 mmol) gradually. After stirring this mixture at room temperature for 4 h, dibromoalkane (10 mmol) and tetrabutyl ammonium bromide (TBAB, 0.32 g, 1.0 mmol) were added to the suspension, and then stirred at 68 °C for 21 h. The solvent was successively removed by distillation at reduced pressure. The resulting residue was washed by ethanol (3×100 mL, 18% in water) to give the colorless powder. The crude product was purified by recrystallization from dichloromethane/hexane (2/1). In this way, the following two compounds were synthesized.

Bipp. (3.2 g, 82%) FT-IR (KBr, ν/cm^{-1}): 3054, 2944, 2883, 1592, 1567, 1491, 1459, 1404, 1230, 1050, 991, 767, 694. 1H NMR (400 MHz, $CDCl_3$, ppm): δ 8.64 (d, 2H, pyridyl H6), 7.94 (d, 2H, pyridyl H3), 7.73 (t, 2H, pyridyl H4), 7.48 (d, 2H, pyrazolyl H5), 7.21 (m, 2H, pyridyl H5), 6.90 (d, 2H, pyrazolyl H3), 4.21 (t, 4H, NCH_2), 2.55 (quintet, 2H, $CH_2CH_2CH_2$). ^{13}C NMR (100 MHz, $CDCl_3$, ppm): δ 152.1 (pyrazolyl C4), 151.9 (pyridyl C2), 149.6 (pyridyl C6), 136.5 (pyrazolyl C5), 131.6 (pyridyl C4), 122.5 (pyridyl C3), 119.8 (pyridyl C5), 104.1 (pyrazolyl C4), 49.3 ($CH_2CH_2CH_2$), 31.0 (NCH_2). MS: m/z ($M + H$)⁺ 331.1673, ($M + Na$)⁺: 353.1454.

Dbnpp. (2.8 g, 85%) FT-IR (KBr, ν/cm^{-1}): 3098, 2951, 2924, 1632, 1593, 1567, 1491, 1457, 1227, 1047, 993, 768, 725, 694. 1H NMR (400 MHz, $CDCl_3$, ppm): δ 8.61 (d, 2H, pyridyl H6), 7.93 (d, 2H, pyridyl H3), 7.69 (t, 2H, pyridyl H4), 7.32 (d, 2H, pyrazolyl H5), 7.29 (m, 2H, pyridyl H5), 7.19 (m, 2H, phenyl H3), 7.15 (t, 2H, phenyl H2), 6.90 (d, 2H, pyrazolyl H3), 5.47 (t, 4H, NCH_2). ^{13}C NMR (400 MHz, $CDCl_3$, ppm): δ 152.3 (pyridyl C6), 151.9 (pyridyl C2), 149.4 (pyrazolyl C4), 136.6 (pyrazolyl C5), 134.7 (pyridyl C4), 130.9 (pyrazolyl C2), 129.5 (phenyl C2), 129.0 (phenyl C3), 122.5 (pyridyl C3), 120.2 (pyridyl C5), 105.1 (pyrazolyl C4), 52.7 (NCH_2). MS: m/z ($M + Na$)⁺ 415.1617.

Eu(III) Complexes. The ligands (0.22 mmol) were dissolved in 10 mL of ethanol. To this solution was added a solution of $Eu(NO_3)_3$.

6H₂O (100 mg, 0.22 mmol) in 5 mL of ethanol. The mixture was then stirred at room temperature for 24 h. The precipitate was filtered, washed with ethanol (3 × 10 mL) and allowed to dry in vacuum for 24 h to afford the complexes as white solid. A saturated solution of Eu(III) complex with Bipp in acetonitrile/acetone/chloroform (1/1/1) was standing with slow evaporation at room temperature. The colorless and transparent crystal appeared in a week.

Solvent Extraction. The organic phase was prepared by dissolving the two ligands and 2-bromohexanoic acid in *tert*-butyl benzene (TBB). The aqueous phase contained HNO₃ of different concentrations and ²⁴¹Am, Eu(III), as well as RE(III) (0.1 mmol/L each). Equal volumes (1.0 mL) of the organic and aqueous phase were stirred in a 5.0 mL round-bottom flask at 25 °C for 60 min. It has been proved that 60 min is sufficient to reach extraction equilibrium (see Figure S15). After phase separation by centrifugation, the concentration of ²⁴¹Am in each phase was measured by a NaI(Tl) scintillation counter. The concentrations of RE(III) in aqueous phase were analyzed by an inductively coupled plasma atomic emission spectrometer (ICP-AES, IRIS Advantage, Thermo Scientific), while those in organic phase were calculated from mass balances by difference between the initial solution and the aqueous phase after extraction. All the extraction experiments were carried out in triplicate. And the mean of three measurements was used to calculate the distribution ratio, which was defined as the ratios of total concentrations of the metal ions in each phase:

$$D_M = [M]_{\text{org}}/[M]_{\text{aq}} \quad (1)$$

The subscripts aq and org represent the aqueous and organic phase, respectively. The separation factors were calculated by the eq 2:

$$SF_{\text{Am/Eu}} = D_{\text{Am}}/D_{\text{Eu}} \quad (2)$$

X-ray Crystallographic Study. A suitable crystal was mounted onto a glass fiber with grease and cooled in a liquid nitrogen stream at 110 K. Crystallographic measurements were made on a New Gemini, Dual, Cu at zero, EosS2 diffractometer. By using Olex2,¹⁶ the structure was solved by Charge Flipping with the Superflip¹⁷ structure solution program and refined with the ShelXL¹⁸ refinement package using Least Squares minimization. All of the non-H atoms were refined anisotropically and the hydrogen atoms were refined by using a riding coordinates. The hydrogen atoms bonded to carbon were included in geometric positions and given thermal parameters equivalent to 1.2 times those of the atom to which they were attached, respectively. In the structure, the hydrogen atoms bonded to oxygen of water molecules could not be located. Crystallographic data are provided in Table S1.

UV-vis Titration. The proper amounts of the ligands were dissolved at desired concentration of 1.0 × 10⁻⁵ mol/L in acetonitrile. The concentration of Eu(NO₃)₃·6H₂O in acetonitrile was 4.0 × 10⁻⁴ mol/L. The 1.0 cm quartz cells were used. The titration was carried out by adding aliquots of 10 μL of Eu(NO₃)₃·6H₂O in acetonitrile into 2 mL of the ligand solution. The pH of the mixed solution was measured to be close to neutral. Background electrolytes were not added to the solution to control the ionic strength. The solution was mixed vigorously for 2 min, which is enough to attain the complexation equilibrium. The stability constants (log K) for Eu(III)–ligands were calculated from the change in the UV-vis absorption spectra of the ligands over the wavelength range of 200–350 nm.

Determination of Stability Constants. The log K of Eu(III) with Bipp and Dbnpp were determined according to the Benesi–Hildebrand equation.¹⁹

$$\frac{1}{A - A_0} = \frac{a}{a - b} \left[\frac{1}{K[M]} + 1 \right] \quad (3)$$

In eq 3, [M] is the concentration of cation; A₀ is the observed absorbance in the absence of M; A is the obtained absorbance with M added. In addition, a and b are constants, logK was evaluated graphically by plotting 1/(A - A₀) vs 1/[M].

Theoretical Methods. All geometry optimizations were carried out with the hybrid B3LYP²⁰ functional implemented in the *Gaussian 09d* program.²¹ For Am(III) and Eu(III), relativistic effects were taken into consideration with the quasi-relativistic effective core potentials (RECPs),²² combining with the corresponding basis sets with a segmented contraction scheme for the valence shells. The electronic configuration of Am(III) and Eu(III) in their septet state was adopted in the calculations of the ground state properties of their complexes. The adopted small-core RECPs replace 60 core electrons for Am(III) and 28 electrons for Eu(III). For all other light atoms, such as C, H, O, and N, the standard Pople-style polarized valence triple- ξ 6-31G(d)²³ basis set was used for optimization and frequency calculations to ensure that the obtained stationary points were the minima on the potential energy surface. All the structures were optimized at the B3LYP/6-31G(d)/RECP level of theory in the gas phase. The polarizable continuum model (PCM)²⁴ was used to take into account solvation effect. The natural atomic charges from the natural population analysis (NPA)²⁵ scheme were calculated at the same level from natural bond orbital (NBO) analyses using the NBO 6.0 version implemented in the *Gaussian 09d* program. The natural atomic charge populations were calculated by natural bond orbital (NBO) analyses at the same method. Multiwfn 3.8²⁶ was used to perform the quantum theory of atoms-in-molecules (QTAIM) analyses of Bader,²⁷ Mayer bond order (MBO), and the charge decomposition analyses (CDA)^{28,29} charge transfer calculation.

To check our calculation reliability, the calculated parameters of [EuL(H₂O)(NO₃)₂]⁺ (L = Bipp) are in fair agreement with our crystal structure discussed above, with a slightly difference of 0.02 Å for Eu–N and 0.06 Å for Eu–O, respectively. Moreover, as stated by Guillaume,³⁰ the increase of basis set size from 6 to 31G(d) to 6-311G(2d,p) at the B3LYP level results in a decrease of the M–L bond lengths by less than 0.01 Å.

RESULTS AND DISCUSSION

Solvent Extraction. Both Bipp and Dbnpp can dissolve in TBB with a solubility of approximate 0.1 mol/L and hardly extract Am(III) and Eu(III) from HNO₃ solution, with the D_{Am} and D_{Eu} being less than 10⁻². Nevertheless, it is fortunate that not only the solubility of Bipp and Dbnpp can reach over 0.25 mol/L in TBB, but also the extraction power for Am(III) and Eu(III) can be enhanced significantly in the presence of 1.0 mol/L 2-bromohexanoic acid. The influence of HNO₃ concentration on the extraction is shown in Figure 2. It is clear that D_{Am} and D_{Eu} decrease with the increase of HNO₃ concentration ranging from 0.001 to 0.1 mol/L. In addition, the

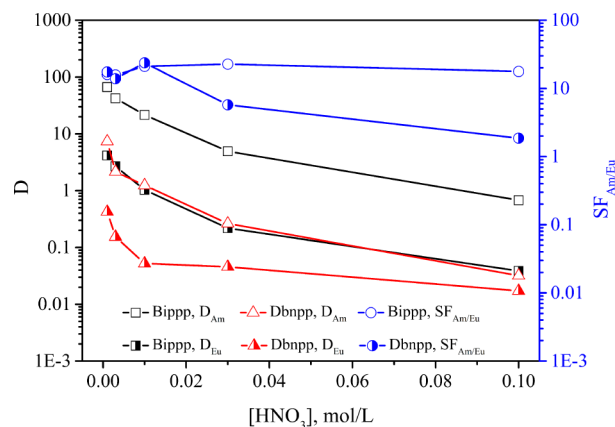


Figure 2. Influence of HNO₃ concentration on the extraction of Am(III) and Eu(III). Organic phase: 0.2 mol/L Bipp or Dbnpp and 1.0 mol/L 2-bromohexanoic acid in TBB; Aqueous phase: tracer amount of ²⁴¹Am or 0.1 mmol/L Eu(NO₃)₃ in HNO₃ solution.

D_M values for Bippp are much higher than those for Dbnpp. The reasons may be the different inductive effects of the alkyl substituents on the N atoms of the pyrazolyl ring. The propyl group of Bippp, having a stronger electron-donating ability than the benzyl group of Dbnpp, increases the extraction efficiency for Am(III) and Eu(III). Besides, as can be seen in Figure 3, it

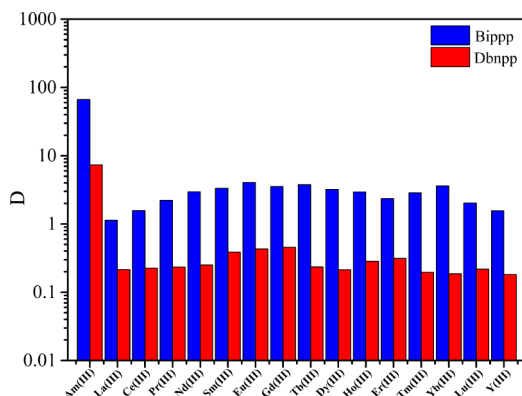


Figure 3. Selectivity of Bippp and Dbnpp for metal ions. Organic phase: 0.2 mol/L Bippp or Dbnpp and 1.0 mol/L 2-bromohexanoic acid in TBB; Aqueous phase: 0.1 mmol/L of each RE(III) or tracer amount of ^{241}Am in 0.001 mol/L HNO_3 solution.

is also possible to selectively separate Am(III) from all RE(III) with $SF_{\text{Am/RE}}$ ranging from 15 to 60. Furthermore, both of the ligands extract the midseries Ln(III), such as Eu(III) and Gd(III), in preference to other RE(III).

To determine the number of ligand molecules present in the extracted complexes, slope analysis was performed. The plot of $\log D_M$ vs $\log [\text{ligand}]_{\text{free}}$ can give a straight line, whose slope represents the number of ligand molecules associated with metal ions. However, due to the difficulty to directly determine the free ligand concentration, an approximate treatment through $[\text{ligand}]_{\text{total}}$ instead of $[\text{ligand}]_{\text{free}}$ is often employed, subject to certain conditions.^{9a,31} It was found that there was no significant difference in pH value of the aqueous phase before and after the extraction equilibrium in the presence of 1.0 mol/L 2-bromohexanoic acid. For example, at the initial aqueous phase pH of 3.06, the equilibrium aqueous phase pH ranged only 2.91–3.03 in the case of 0.01–0.25 mol/L Bippp or Dbnpp. This indicates that both Bippp and Dbnpp are not easily protonated under the above-mentioned experimental conditions. In other words, the organic phase hardly extracts HNO_3 at the initial pH of ~ 3 . And meanwhile, the ligand concentration of 0.01–0.25 mol/L is much higher than that of Am(III) and Eu(III). $[\text{ligand}]_{\text{free}}$ is approximately equal to $[\text{ligand}]_{\text{total}}$. Therefore, the plots of $\log D_M$ vs $\log [\text{ligand}]_{\text{total}}$ can be comparable to those of $\log D_M$ vs $\log [\text{ligand}]_{\text{free}}$. Figure 4 shows the influence of the ligand concentration on the extraction of Am(III) and Eu(III). All of the obtained slope values are not the integers. The main reasons for this result may be as follows. On one hand, some commonly used approximate treatments, such as concentration instead of thermodynamic activity and $[\text{ligand}]_{\text{total}}$ instead of $[\text{ligand}]_{\text{free}}$ can cause this deviation. On the other hand, for an extraction system of *N*-donor heterocyclic ligands and carboxylic acid, it has been shown that there may be an organic complex forming between these two types of organic molecules,³¹ resulting in the noninteger discrepancy. In particular, the slope values of Bippp are 1.43 and 1.25 for Am(III) and Eu(III), respectively, which

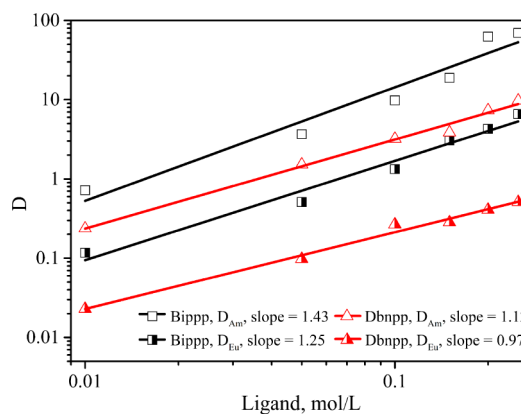


Figure 4. Influence of ligand concentration on the extraction of Am(III) and Eu(III). Organic phase: 0.01–0.25 mol/L Bippp or Dbnpp and 1.0 mol/L 2-bromohexanoic acid in TBB; Aqueous phase: tracer amount of ^{241}Am or 0.1 mmol/L $\text{Eu}(\text{NO}_3)_3$ in 0.001 mol/L HNO_3 solution.

are significantly higher than 1. This would suggest the formation of 1:1 and 1:2 metal:ligand complexes. Nevertheless, owing to the values being closer to 1 rather than 2, it could be inferred that the 1:1 complexes of the ligands with Am(III) and Eu(III) in solvent extraction are dominant, while the 1:2 ones are nondominant. Similar results were also reported for the extraction of Am(III) and Eu(III) by C5-BTBP and nonanoic acid in *tert*-butylbenzene.³² And meanwhile, it was supported by the subsequent experiments of X-ray diffraction, UV–vis titration, and MS, too.

Structures of Eu(III) Complexes. Great efforts were made to prepare single crystals of Eu(III) complexes with Bippp and with Dbnpp. The single crystal of Eu(III) complex with Bippp was obtained by slow evaporation in acetone/acetonitrile/chloroform (1/1/1). Unfortunately, the single crystal of Eu(III) complex with Dbnpp was not obtained. As displayed in Figure 5, Bippp is bound to Eu(III) through two N atoms of pyrazolyl rings together with two other N atoms of pyridyl rings. Interestingly, the Eu–N bond lengths of the pyrazolyl N atoms (average length 2.542 Å; see Table S2) are slightly shorter than those for the pyridyl N atoms (average length 2.560 Å; see

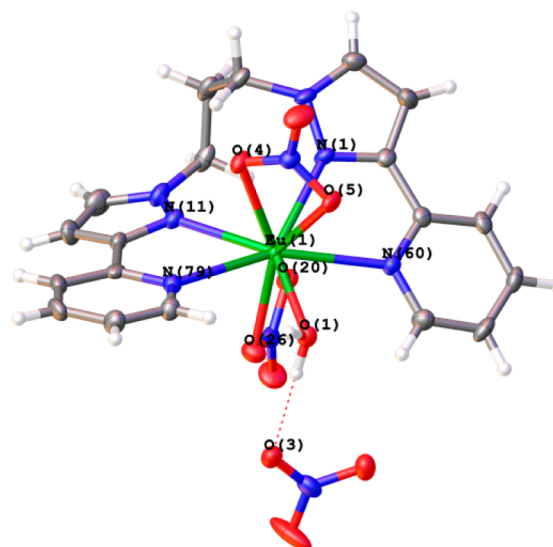


Figure 5. Single crystal structure of the Eu(III) complex with Bippp.

Table S2), suggesting that pyrazolyl rings are more likely to coordinate with Eu(III) than pyridyl rings. This observation will be investigated deeply in DFT calculations. In addition, the two nitrate ions are bound to the Eu(III) center. The Eu–O bond lengths of nitrate ions are within the expected range of 2.464–2.559.^{12,13} The difference between two Eu–O bond lengths for each coordinated nitrate ion is small, so nitrate ions could coordinate with Eu(III) in a symmetric bidentate manner.³³ Like the Eu(III) complex with dmpbipy, one water molecule also participates in coordination. And the two Eu(III) complexes do not reveal any obvious differences in their Eu–O bond lengths.¹² Outside the primary coordination, one free nitrate ion is hydrogen bonded to the water molecule coordinated with Eu(III) to keep the charge balance. This can also be observed in the FT-IR spectrum of the Eu(III) complex with Bippp (see Figure S3). A strong and sharp peak at 1384 cm⁻¹ represents the vibration of the free nitrate ion. Moreover, Figure S11 and S12 give the MS spectra of the Eu(III) complexes with Bippp and Dbnpp. The high intensity peaks at $m/z = 607.0510$ and 669.0667 represent two different molecular species, denoting the complexes of [Eu(Bippp)(NO₃⁻)₂]⁺ and [Eu(Dbnpp)(NO₃⁻)₂]⁺, respectively. The isotope distribution patterns of these peaks (see Figure S13 and S14) are in accordance with those by computer simulation for the 1:1 complexes. These results clearly demonstrate that the metal ion binds with only one Bippp molecule, which agrees well with X-ray crystallographic and slope analysis results.

Solution Spectroscopy. The complexation behavior of each ligand with Eu(III) was investigated by UV–vis titration. The changes in the absorption spectra of ligands as a function of the Eu(III) concentration in acetonitrile are given in Figure 6. As Eu(III) concentration increased, the absorbance of ligands at 252 nm decreased. The new peak at 289 nm corresponding to the M–L complex is also presented. The increase in the absorption intensity for the new peak with the addition of Eu(III) is also observed. Moreover, there are two isosbestic points on every titration curve, which confirms that only one type of complex is formed upon the addition of Eu(III).

As can be seen in Figure S16, the plots of $1/(A-A_0)$ at 252 nm vs $1/[Eu(III)]$ give two straight lines (correlation coefficient: $R^2 = 0.995$ for Bippp; 0.999 for Dbnpp), indicating that the 1:1 Eu(III) complexes with Bippp and Dbnpp are formed in solution, separately. The results are in line with that observed in MS spectra and the slope analyses of extraction. The calculated log K values for Eu(III) with Bippp and Dbnpp are 4.75 ± 0.03 and 4.45 ± 0.04 , respectively. As far as log K is concerned, it is clear that the complexation abilities of Bippp and Dbnpp are similar to those of other N-donor heterocyclic ligands, such as ADPTZ, C5-hemi-BTP and C5-BTBP.³⁴ The log K for the Bippp complex is higher than that for the Dbnpp complex, which is consistent with the higher D_{Eu} for Bippp observed in the extraction.

DFT Calculations. In general, 2-bromohexanoic acid is believed to improve the lipophilicity of the extracted complexes.¹³ However, it is still a priori unknown how it interacts with the metal ions. As a relatively “softer” anion, if 2-bromohexanoic acid has the chance to form an inner sphere complex with the metal ions, it has to compete against the nitrate ion, which is a relatively “harder” anion with stronger affinity to bind with An(III)/Ln(III). In other words, the nitrate ion plays a more important role in the formation of M–L complexes than 2-bromohexanoic acid. Thus, we considered

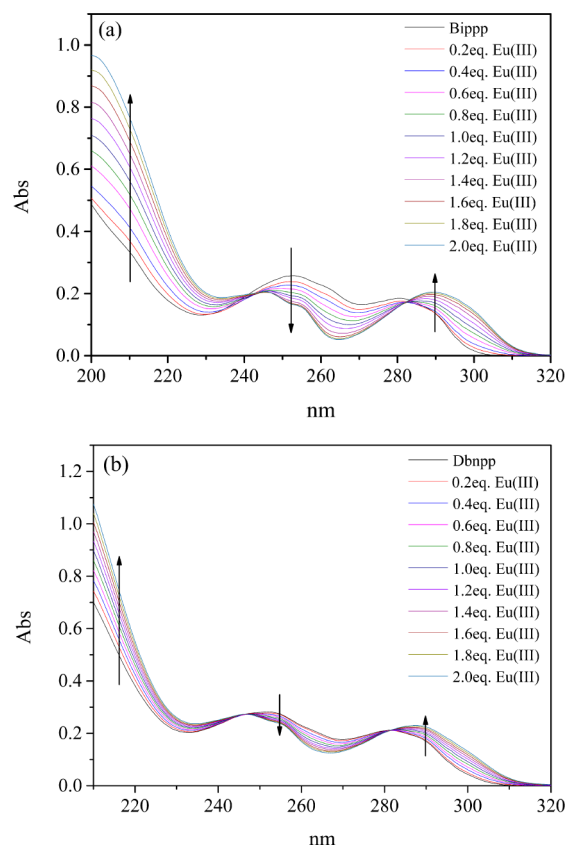


Figure 6. UV–vis absorption spectroscopic titration of Bippp (a) and Dbnpp (b) with Eu(NO₃)₃·6H₂O in acetonitrile (initial conditions, [ligand] = 1.0×10^{-5} mol/L, volume = 2.0 mL; titration conditions, [Eu(NO₃)₃·6H₂O] = 4.0×10^{-4} mol/L).

only the inner sphere complex formation of nitrate ion rather than the 2-bromohexanoic acid. In this work, the structures of neutral ML(NO₃)₃ complexes (M = Am(III), Eu(III); L = Bippp, Dbnpp) were optimized and their thermodynamic stabilities were compared in both the gas phase and water.

Complex Formation Energies. The calculated binding energies of ML(NO₃)₃ and ΔE (ΔG), and the differences in the energies, $\Delta(\Delta X_{cf})_{Am/Eu}$ ($X = E$ (G)), of formation of two analogous complexes of Am(III) and Eu(III) in both the gas phase and water were summarized in Table 1. As expected, the Bippp chelated complexes are more stable than the corresponding Dbnpp complexes in both the gas phase and water. The EuL(NO₃)₃ complexes are more stable than the corresponding AmL(NO₃)₃ complexes with bare M³⁺ as substrate in the gas phase ($\Delta(\Delta E_{cf})_{Am/Eu} = +51$ kJ/mol). In contrast, when the solvent effect is taken into account, the above relation changes to the opposite. When changing to M(H₂O)₉³⁺ as substrate, the $\Delta(\Delta E_{cf})_{Am/Eu}$ values are equal to -12 kJ/mol in the gas and -18 kJ/mol in the aqueous medium (PCM), respectively. This phenomenon had been well interpreted by Narbutt et al.³⁵ They had compared the differences in the energies, $\Delta(\Delta E_{cf})_{Am/Eu}$, of formation of BTBP complexes of M³⁺ cations in the gas phase and water (-0.13 and -13.1 kJ/mol, respectively). These results imply that the selectivity of Bippp and Dbnpp for Am(III) over Eu(III) is comparable to that of the BTBP ligands.

In order to further explore the influence of ligands structure on complexation reactions, the deformation energy (ΔE_{deform}) was calculated in the gas phase. ΔE_{deform} was defined as the

Table 1. Complex Formation Energies and Gibbs Free Energies, kJ/mol, of the ML(NO₃)₃ Complexes and the Differences in the Energies and Gibbs Free Energies, $\Delta(\Delta X_{cf})_{Am/Eu}$ ($X = E(G)$), of Formation of Bipp and Dbnpp Complexes of Am³⁺ and Eu³⁺ in the Gas Phase and Water (PCM), Calculated at the B3LYP/6-31G(d)/RECP Level

ML(NO ₃) ₃	Metal ion	Phase	ΔE_{cf}	ΔG_{cf}	$\Delta(\Delta E_{cf})_{Am/Eu}$	$\Delta(\Delta G_{cf})_{Am/Eu}$	
Bipp	Eu	M ³⁺	Gas	-4540.1	-4305.9		
		M(H ₂ O) ₉ ³⁺	Gas	-2071.9	-2260.8		
		M(H ₂ O) ₉ ³⁺	H ₂ O	-25.1	-219.9		
	Am	M ³⁺	Gas	-4488.7	-4254.8	+51.4	+51.1
		M(H ₂ O) ₉ ³⁺	Gas	-2084.0	-2269.6	-12.1	-8.8
		M(H ₂ O) ₉ ³⁺	H ₂ O	-42.9	-241.0	-17.8	-21.1
Dbnpp	Eu	M ³⁺	Gas	-4517.1	-4285.6		
		M(H ₂ O) ₉ ³⁺	Gas	-2048.9	-2240.5		
		M(H ₂ O) ₉ ³⁺	H ₂ O	-0.5	-195.6		
	Am	M ³⁺	Gas	-4465.9	-4234.2	+51.2	+51.4
		M(H ₂ O) ₉ ³⁺	Gas	-2061.2	-2249.0	-12.3	-8.5
		M(H ₂ O) ₉ ³⁺	H ₂ O	-18.8	-216.9	-18.3	-21.3

Table 2. Calculated M–N and M–O Distances (d_{M-X} , in Å), MBO, and BOP in ML(NO₃)₃ Complexes in the Gas Phase

ML(NO ₃) ₃	Eu						Am					
	Bipp			Dbnpp			Bipp			Dbnpp		
	N _{py}	N _{pz}	O									
<i>d</i> (Å)	2.72	2.74	2.49	2.72	2.78	2.48	2.72	2.77	2.52	2.72	2.80	2.52
MBO	0.22	0.20	0.29	0.23	0.19	0.29	0.22	0.20	0.32	0.23	0.19	0.32
BOP	0.17	0.18	0.20	0.18	0.17	0.20	0.17	0.17	0.23	0.17	0.16	0.23

Table 3. QTAIM Analyses of Electron Density, ρ_c (e⁻/Bohr³), Laplacian, $\nabla^2\rho_b$ (e⁻/Bohr⁵), and Energy Density, H_c (a.u.), at the Critical Points of M–N Bonds in ML(NO₃)₃ Complexes

ML(NO ₃) ₃	EuBipp		EuDbnpp		AmBipp		AmDbnpp	
	N _{py}	N _{pz}						
rN/rM	1.32/1.40	1.33/1.43	1.32/1.40	1.35/1.44	1.29/1.44	1.30/1.47	1.29/1.43	1.31/1.48
ρ_c	0.030	0.025	0.030	0.024	0.034	0.028	0.034	0.027
$\nabla^2\rho_b$	0.092	0.088	0.090	0.083	0.106	0.099	0.106	0.094
H_c	0.0006	0.0019	0.0005	0.0017	-0.0003	0.0008	-0.0003	0.0008

energy difference between the ligands in the ML(NO₃)₃ complexes and the free ligands (see Table S3). It can be seen that complexes formed with Bipp (20 kJ/mol) require smaller deformation energy compared with the Dbnpp (27 kJ/mol) cases. In other words, these results indicate that the orbital interaction of preorganized ligands with the metal ions must dominate the complexation reactions. The following electronic structure studies would shed light on these points.

Electronic Structures. The relevant structural parameters of ML(NO₃)₃ complexes are shown in Table 2, i.e. bond lengths (*d*), Mayer bond order (MBO), and the bond overlap populations (BOP). The M–L (M–N_{py} and M–N_{pz}) and metal–oxygen (nitrate ions) bond lengths are given as averaged. The M–N_{py} bond lengths are shorter than the M–N_{pz} bond lengths in both Bipp and Dbnpp complexes. Accordingly, the bond orders of M–N_{py} are higher than those of M–N_{pz}. It should be noted that this relation is opposite to the experimental values (see Table S2), but this is quite understandable. First, the coordination number (CN) of Eu³⁺ in the crystal structure [EuL(NO₃)₂(H₂O)][NO₃] (L = Bipp) is nine, whereas the CN of computational model EuL(NO₃)₃ (L = Bipp) is ten. Moreover, one water molecule in the crystal structure is instead replaced by one nitrate ion in the structure optimization of EuL(NO₃)₃. All these tiny differences may lead to the discrepancy. In addition, the structure of [EuL(NO₃)₂(H₂O)]⁺ has been optimized as well. The M–N_{pz}

bond length is 2.61 Å, which is shorter than that of M–N_{py} (2.63 Å). These are fairly comparable with the experimental results. Generally, all the BOP values are very small, implying a minor covalent contribution and a strong ionic character of all the M–N bonds. Moreover, the MBO values are about 0.3 for Am(III) and 0.2 for Eu(III), respectively. It is likely that the ionic interaction may dominate the M–L interaction in ML(NO₃)₃ complexes. This is in good agreement with the following charge transfer analyses.

Detailed analyses of M–L interactions were also carried out using the QTAIM method. This topological method could well probe the covalence in *f*-element–ligand bonds.³⁶ The electron density (ρ_c), Laplacian ($\nabla^2\rho_b$), and energy densities (H_c) data at the bond critical points (BCPs) of M–N bonds for ML(NO₃)₃ complexes are listed in Table 3. The ρ_c values of all corresponding M–N bonds for Am(III) complexes are a little higher than that for the Eu(III) complexes, indicating that the bonds in the former are more covalent. Moreover, the M–N_{pz} bonds show more covalent feature than the M–N_{py} ones. Similar trends on the covalence of M–N bonds in both Bipp and Dbnpp result from the analysis of Laplacian values at their BCPs. The positive $\nabla^2\rho_b$ values demonstrate the domination of closed-shell interactions between the metal ions and donor N atoms. This is confirmed by the energy density H_c values which are close to zero, and consistent with the low MBOs and BOPs discussed in the previous section.

Table 4. NPA Charges on Selected Atoms in the Free Ligands and in the Corresponding $\text{ML}(\text{NO}_3)_3$ Complexes ($\text{M} = \text{Eu}$ and Am , $\text{L} = \text{Bipp}$ and Dbnpp), and the Differences between the Charges on the Corresponding Fragments (py and pz) of the Ligand in the Given Complexes and in the Free Ligands, Δq_{py} and Δq_{pz}

Compd	M	py	N_{py}	Δq_{py}	pz	N_{pz}	Δq_{pz}	NO_3
Bipp		-0.026	-0.440		-0.245	-0.274		
$\text{EuL}(\text{NO}_3)_3$	1.66	0.083	-0.490	0.11	-0.171	-0.316	0.07	-0.535
$\text{AmL}(\text{NO}_3)_3$	1.68	0.083	-0.500	0.11	-0.172	-0.321	0.07	-0.541
Dbnpp		-0.026	-0.441		-0.231	-0.273		
$\text{EuL}(\text{NO}_3)_3$	1.66	0.083	-0.489	0.11	-0.160	-0.321	0.07	-0.536
$\text{AmL}(\text{NO}_3)_3$	1.68	0.083	-0.501	0.11	-0.160	-0.323	0.07	-0.540

Charge Transfer in the Complexes. As listed in Table 4, the average charges on ligand fragments, particular ligand atoms, and the metal ions in the $\text{ML}(\text{NO}_3)_3$ coordination complexes were calculated via NPA scheme. The calculation shows significant ligand-to-metal charge transfer (MLCT), which decreases the +3 formal charge of chelated metal ions. In the free Bipp and Dbnpp ligands, the group charges of the pyridyl (py) rings are negative and close to zero ($-0.026 e^-$). In contrast, the charges of the pyrazolyl (pz) rings are more negative (from -0.231 to $-0.245 e^-$). These suggest that the pz rings may act as better electron donors than py rings. Actually, the shifts of electron density on the metal ions from pz rings ($\Delta q_{\text{pz}} = 0.07 e^-$) are smaller than that from py rings ($\Delta q_{\text{py}} = 0.11 e^-$), but both of them are not very large. This may ascribe to the induced polarization of ligands by the coordinated metal ions. The shifts of atomic charge on Eu(III) and Am(III) remain as 1.34 and $1.32 e^-$, respectively, which indicating that there may exist covalent character in M–L bonding. It should be noted that Am(III) (1.68) show more positive charges than Eu(III) (1.66) in $\text{ML}(\text{NO}_3)_3$ complexes. It should be noted that the greater shifts of electron density to the Eu(III) than the Am(III) cation agree with those revealed by Lan et al.³⁷ whereas remain in contrast to those reported by Narbutt et al.³⁵

Besides the above charge distribution analyses, the charge decomposition analysis (CDA) and extended charge decomposition analyses (ECDA) methods are also applied to examine how the charge is transferred between the metal ions and ligand fragments. The data were collected in Table S4. The net charge transfer from Bipp complexes is slightly smaller than that in the corresponding Dbnpp complexes. It is also worth noting that the net charge transfer from nitrate ions to metal ions is much greater than that from the N-rich ligands.

CONCLUSIONS

The two pyridylpyrazole based tetradentate ligands were synthesized as the extractants of Am(III) and Eu(III). These ligands exhibited good selectivity for Am(III) over Eu(III) and other RE(III) in HNO_3 solution. Slope analyses showed that the two ligands extracted Am(III) and Eu(III) as 1:1 complexes in the presence of 2-bromohexanoic acid, which is also confirmed by X-ray crystallography and MS analyses. UV–vis titration analyses indicated that Bipp had stronger affinity for Eu(III) than Dbnpp, which is in good accordance with the solvent extraction results. The QTAIM analyses showed that the Am–N bonds are more covalent compared with the Eu–N bonds. The NPA and CDA analysis suggested that charge transfer is the main reason responsible for stabilization of the $\text{ML}(\text{NO}_3)_3$ complexes and shows a strong ionic character of the M–ligand bonds. This is in line with the results of the MBO and BOP analysis. Although the extraction performance of the two pyridylpyrazole based tetradentate ligands is not sufficient

to meet the practical needs for Ans(III)/Lns(III) separation, e.g. relatively low $SF_{\text{Am/RE}}$ and the necessity to use 2-bromohexanoic acid as a counterion in the extraction system, the results of this paper would provide important guidance to design improved extractants for An(III)/Ln(III) separation in the future.

ASSOCIATED CONTENT

Supporting Information

The Supporting Information is available free of charge on the ACS Publications website at DOI: 10.1021/acs.inorgchem.5b01452.

Characterization data of all compounds, UV–vis absorption, selected bond lengths/angles of Eu(III) complex with Bipp, and structure of Eu(III) complex with Bipp in the CSD database (PDF)

X-ray crystallographic data of Eu(III) complex with Bipp (CIF)

AUTHOR INFORMATION

Corresponding Authors

*E-mail: dsd68@163.com.

*E-mail: chuang@scu.edu.cn.

Notes

The authors declare no competing financial interest.

ACKNOWLEDGMENTS

The authors are very grateful for the financial support by the National Natural Science Foundation of China (Nos. 91126016, 91426302, 91226105, and J1210004). The comprehensive training platform of specialized laboratory, College of Chemistry, Sichuan University, is acknowledged for NMR, MS, ICP-AES, and X-ray diffraction analyses.

REFERENCES

- (1) (a) Denniss, I. S.; Jeapes, A. P. In *The Nuclear Fuel Cycle*; Wilson, P. D., Ed.; Oxford University Press: Oxford, U.K., 1986; pp 116–132. (b) Nash, K. L.; Choppin, G. R. *Sep. Sci. Technol.* **1997**, *32*, 255–274.
- (2) Sood, D. D.; Patil, S. K. *J. Radioanal. Nucl. Chem.* **1996**, *203*, 547–573.
- (3) (a) Magill, J.; Berthou, V.; Haas, D.; Galy, J.; Schenkel, R.; Wiese, H.-W.; Heusener, G.; Tommasi, J.; Youinou, G. *Nucl. Energy* **2003**, *42*, 263–277. (b) Salvatores, M.; Palmiotti, G. *Prog. Part. Nucl. Phys.* **2011**, *66*, 144–166.
- (4) Mathur, J. N.; Murali, M. S.; Nash, K. L. *Solvent Extr. Ion Exch.* **2001**, *19*, 357–390.
- (5) Pearson, R. G. *J. Am. Chem. Soc.* **1963**, *85*, 3533–3539.
- (6) Nash, K. L. *Solvent Extr. Ion Exch.* **1993**, *11*, 729–768.
- (7) (a) Musikas, C.; LeMarois, G.; Fittoussi, R.; Cuillerdier, C. Properties and uses of nitrogen and sulfur donor ligands in actinide separations. In *Actinide Separations*; Navratil, J. D., Schulz, W. W., Eds.;

- ACS Symposium Series 117; American Chemical Society: Washington, DC, 1980; p 130. (b) Jensen, M. P.; Bond, A. H. *J. Am. Chem. Soc.* **2002**, *124*, 9870–9877. (c) Dam, H. H.; Reinhoudt, D. N.; Verboom, W. *Chem. Soc. Rev.* **2007**, *36*, 367–377. (d) Kolarik, Z. *Chem. Rev.* **2008**, *108*, 4208–4252.
- (7) Zhu, Y. *Radiochim. Acta* **1995**, *68*, 95–98.
- (8) Modolo, G.; Odoj, R. *Solvent Extr. Ion Exch.* **1999**, *17*, 33–53.
- (9) (a) Kolarik, Z.; Müllich, U.; Gassner, F. *Solvent Extr. Ion Exch.* **1999**, *17*, 23–32. (b) Kolarik, Z.; Müllich, U.; Gassner, F. *Solvent Extr. Ion Exch.* **1999**, *17*, 1155–1170. (c) Denecke, M. A.; Rossberg, A.; Panak, P. J.; Weigl, M.; Schimmelpfennig, B.; Geist, A. *Inorg. Chem.* **2005**, *44*, 8418–8425.
- (10) (a) Foreman, M. R. S.; Hudson, M. J.; Drew, M. G. B.; Hill, C.; Madic, C. *Dalton Trans.* **2006**, 1645–1653. (b) Steppert, M.; Císářová, I.; Fanghänel, T.; Geist, A.; Lindqvist-Reis, P.; Panak, P.; Štěpnička, P.; Trumm, S.; Walther, C. *Inorg. Chem.* **2012**, *51*, 591–600.
- (11) Lewis, F. W.; Harwood, L. M.; Hudson, M. J.; Drew, M. G. B.; Desreux, J. F.; Vidick, G.; Bouslimani, N.; Modolo, G.; Wilden, A.; Sypula, M.; Vu, T. H.; Simonin, J. P. *J. Am. Chem. Soc.* **2011**, *133*, 13093–13102.
- (12) Girt, D.; Roesky, P. W.; Geist, A.; Ruff, C. M.; Panak, P. J.; Denecke, M. A. *Inorg. Chem.* **2010**, *49*, 9627–9635.
- (13) Bremer, A.; Ruff, C. M.; Girt, D.; Müllich, U.; Rothe, J.; Roesky, P. W.; Panak, P. J.; Karpov, A.; Müller, T. J. J.; Denecke, M. A.; Geist, A. *Inorg. Chem.* **2012**, *51*, 5199–5207.
- (14) Adam, C.; Beele, B. B.; Geist, A.; Müllich, U.; Kaden, P.; Panak, P. J. *Chem. Sci.* **2015**, *6*, 1548–1561.
- (15) Brunner, H.; Scheck, T. *Chem. Ber.* **1992**, *125*, 701–709.
- (16) Dolomanov, O. V.; Bourhis, L. J.; Gildea, R. J.; Howard, J. A. K.; Puschmann, H. *J. Appl. Crystallogr.* **2009**, *42*, 339–341.
- (17) (a) Palatinus, L.; Chapuis, G. *J. Appl. Crystallogr.* **2007**, *40*, 786–790. (b) Palatinus, L.; Van Der Lee, A. *J. Appl. Crystallogr.* **2008**, *41*, 975–984. (c) Palatinus, L.; Prathapa, S. J.; van Smaalen, S. *J. Appl. Crystallogr.* **2012**, *45*, 575–580.
- (18) Sheldrick, G. M. *J. Acta Crystallogr., Sect. A: Found. Crystallogr.* **2008**, *64*, 112–122.
- (19) (a) Benesi, H. A.; Hildebrand, J. H. *J. Am. Chem. Soc.* **1949**, *71*, 2703–2707. (b) Barra, M.; Bohne, C.; Scaiano, J. C. *J. Am. Chem. Soc.* **1990**, *112*, 8075–8579.
- (20) (a) Lee, C.; Yang, W.; Parr, R. G. *Phys. Rev. B: Condens. Matter Mater. Phys.* **1988**, *37*, 785–789. (b) Becke, A. D. *J. Chem. Phys.* **1993**, *98*, 5648–5652.
- (21) Frisch, M. J.; Trucks, G. W.; Schlegel, H. B.; Scuseria, G. E.; Robb, M. A.; Cheeseman, J. R.; Scalmani, G.; Barone, V.; Mennucci, B.; Petersson, G. A.; Nakatsuji, H.; Caricato, M.; Li, X.; Hratchian, H. P.; Izmaylov, A. F.; Bloino, J.; Zheng, G.; Sonnenberg, J. L.; Hada, M.; Ehara, M.; Toyota, K.; Fukuda, R.; Hasegawa, J.; Ishida, M.; Nakajima, T.; Honda, Y.; Kitao, O.; Nakai, H.; Vreven, T.; Montgomery, J. A.; Peralta, J. E.; Ogliaro, F.; Bearpark, M.; Heyd, J. J.; Brothers, E.; Kudin, K. N.; Staroverov, V. N.; Kobayashi, R.; Normand, J.; Raghavachari, K.; Rendell, A.; Burant, J. C.; Iyengar, S. S.; Tomasi, J.; Cossi, M.; Rega, N.; Millam, J. M.; Klene, M.; Knox, J. E.; Cross, J. B.; Bakken, V.; Adamo, C.; Jaramillo, J.; Gomperts, R.; Stratmann, R. E.; Yazyev, O.; Austin, A. J.; Cammi, R.; Pomelli, C.; Ochterski, J. W.; Martin, R. L.; Morokuma, K.; Zakrzewski, V. G.; Voth, G. A.; Salvador, P.; Dannenberg, J. J.; Dapprich, S.; Daniels, A. D.; Farkas, Ö.; Foresman, J. B.; Ortiz, J. V.; Cioslowski, J.; Fox, D. J. *Gaussian 09*, revision D.01; Gaussian, Inc.: Wallingford, CT, 2009.
- (22) (a) Cao, X. Y.; Dolg, M.; Stoll, H. *J. Chem. Phys.* **2003**, *118*, 487–496. (b) Küchle, W.; Dolg, M.; Stoll, H.; Preuss, H. *J. Chem. Phys.* **1994**, *100*, 7535–7542.
- (23) Hariharan, P. C.; Pople, J. A. *Theor. Chim. Acta* **1973**, *28*, 213–222.
- (24) Tomasi, J.; Mennucci, B.; Cammi, R. *Chem. Rev.* **2005**, *105*, 2999–3093.
- (25) Reed, A. E.; Weinstock, R. B.; Weinhold, F. *J. Chem. Phys.* **1985**, *83*, 735–746.
- (26) Lu, T.; Chen, F. W. *J. Comput. Chem.* **2012**, *33*, 580–592.
- (27) (a) Bader, R. F. W. *Atoms in Molecules. A Quantum Theory*; Clarendon Press; Clarendon Press: Oxford, U.K., 1994. (b) Popelier, P. *Atoms in Molecules: An Introduction*; Prentice Hall: Harlow, 2000.
- (28) Dapprich, S.; Frenking, G. *J. Phys. Chem.* **1995**, *99*, 9352–9362.
- (29) Gorelsky, S. I.; Ghosh, S.; Solomon, E. I. *J. Am. Chem. Soc.* **2006**, *128*, 278–290.
- (30) Guillaumont, D. *J. Phys. Chem. A* **2004**, *108*, 6893–6900.
- (31) Hagström, I.; Spjuth, L.; Enarsson, Å.; Liljenzin, J. O.; Skälberg, M.; Hudson, M. J.; Ivesonb, P. B.; Madic, C.; Cordier, P. Y.; Hill, C.; Francois, N. *Solvent Extr. Ion Exch.* **1999**, *17*, 221–242.
- (32) Nilsson, M.; Andersson, S.; Drouet, F.; Ekberg, C.; Foreman, M.; Hudson, M.; Liljenzin, J. O.; Magnusson, D.; Skarnemark, G. *Solvent Extr. Ion Exch.* **2006**, *24*, 299–318.
- (33) Jones, P. L.; Amoroso, A. J.; Jeffery, J. C.; McCleverty, J. A.; Psillakis, E.; Rees, L. H.; Ward, M. D. *Inorg. Chem.* **1997**, *36*, 10–18.
- (34) (a) Miguiditchian, M.; Guillaneux, D.; Guillaumont, D.; Moisy, P.; Madic, C.; Jensen, M. P.; Nash, K. L. *Inorg. Chem.* **2005**, *44*, 1404–1412. (b) Hubscher-Bruder, V.; Haddaoui, J.; Bouhroum, S.; Arnaud-Neu, F. *Inorg. Chem.* **2010**, *49*, 1363–1371.
- (35) Narbutt, J.; Oziminskia, W. P. *Dalton Trans.* **2012**, *41*, 14416–14424.
- (36) (a) Jones, M. B.; Gaunt, A. J.; Gordon, J. C.; Kaltsoyannis, N.; Neu, M. P.; Scott, B. L. *Chem. Sci.* **2013**, *4*, 1189–1203. (b) Schnaars, D. D.; Gaunt, A. J.; Hayton, T. W.; Jones, M. B.; Kirker, I.; Kaltsoyannis, N.; May, I.; Reilly, S. D.; Scott, B. L.; Wu, G. *Inorg. Chem.* **2012**, *51*, 8557–8566. (c) Arnold, P. L.; Turner, Z. R.; Kaltsoyannis, N.; Pelekanaki, P.; Bellabarba, R. M.; Tooze, R. P. *Chem. - Eur. J.* **2010**, *16*, 9623–9629. (d) Vlaisavljevich, B.; Miró, P.; Cramer, C. J.; Gagliardi, L.; Infante, I.; Liddle, S. T. *Chem. - Eur. J.* **2011**, *17*, 8424–8433.
- (37) Lan, J. H.; Shi, W. Q.; Yuan, L. Y.; Zhao, Y. L.; Li, J.; Chai, Z. F. *Inorg. Chem.* **2011**, *50*, 9230–9237.